EFFECT OF SILICON CONTENT ON CARBIDE PRECIPITATION AND LOW TEMPERATURE TOUGHNESS OF THE PRESSURE VESSEL STEELS

L.H. Ruan[1], K.M. Wu[1]*, J.A. Qiu[1], Irina Rodionova[2], A. A. Shirzadi[1,3,4]

[1]The State Key Laboratory of Refractories and Metallurgy, Hubei Province Key Laboratory of Systems Science in Metallurgical Process, International Research Institute for Steel Technology, Wuhan University of Science and Technology, Wuhan 430081, China

[2]Center of physical chemistry, materials science, bimetals and special forms of corrosion (CPMC), I. P. Bardin Central Research Institute for Ferrous Metallurgy, Moscow, 105005, Russian Federation

[3]Department of Engineering and Innovation, The Open University, Walton Hall, Milton Keynes, MK7 6AA, UK

[4]Department of Materials Science and Metallurgy, University of Cambridge, 27 Charles Babbage Road, Cambridge CB3 0FS, UK

* Corresponding author: K.M. Wu

Tel.: +86 27 68862772; fax: +86 27 68862606

E-mail address: wukaiming@wust.edu.cn, 1052516931@qq.com

ABSTRACT

The effect of silicon content (0.54 and 1.55 wt.% Si) on carbide precipitation and low temperature toughness of Cr-Mo alloyed pressure vessel steels was investigated in this work. Microstructural examinations showed that both steels consisted of bainite and ferrite, after normalizing at 1000 ºC for 30 mins followed by tempering at 650 and 700 ºC for 180 mins. The average room temperature toughness decreased from 158 to 83 J and average size of carbides increased from 20~30 nm to 40~60 nm as the silicon content increased from 0.54 to 1.55 wt.%. Fine M_6C and $M_{23}C_6$ carbides were found in the 0.54 % Si steel, whereas coarser M_7C_3 and $M_{23}C_6$ carbides were observed in the 1.55 % Si steel. The results of this work suggested that cementite was precipitated in the early stage of tempering in the low silicon steel. Then, fine dispersed Cr-Mo carbides were nucleated on the preformed cementite precipitates. These fine alloy carbides were accounted for the improved low-temperature impact toughness of the low silicon steel.

Key words**:** pressure vessel steels, silicon, toughness, carbides, Cr-Mo steels.

INTRODUCTION

Cr-Mo type low-alloy steels are widely used in the power generation and petrochemical industries as structural materials, mostly due to their high toughness at low temperatures while maintaining high strengths at elevated temperatures. Unfortunately, when subjected to intermediate service temperatures for long times, these steels suffer reduction in fracture toughness as well as rise in their ductile-to-brittle transition temperatures [1-5]. Two main factors responsible for the loss of toughness and premature failure are changes in the micro-chemistry of grain boundaries (referred to as *temper embrittlement*) [6-8], and precipitation of alloy carbides *e.g.* $M_{23}C_6$, M_6C and M_7C_3 [9-11]. Some recent works showed that long service times lead to overgrown alloy carbides, which can no longer pin down the dislocations or prevent grain/lath boundaries migration; resulting in premature fractures [12]. Therefore, by refining alloy carbides or retarding their growth it might be possible to extend the service life of this family of steels.

Tempering is an important and widely used heat treatment for high-strength low-alloy steels as the precipitation of fine alloy carbides during tempering can contribute to higher strength and toughness [13, 14]. Silicon is one of the main alloying elements and very effective in refining carbides by delaying the conversion of ε-carbide to cementite during tempering cycles [15]. It is reported that reduction in silicon content could increase the toughness of medium carbon quenched-tempered Cr-Mo alloy steels due to its ability in altering the nature and distribution of alloy carbides [16, 17]. More recent work indicated that silicon can reduce the size of Nb-Ti carbides, precipitated in a cryogenic pressure vessel steels, and hence increased their ultra-low temperature toughness [18]. However, the correlation between silicon content and the dispersion of alloy carbides is not well understood. The effect of Si on carbide precipitation and low temperature impact toughness of tempered Cr-Mo steels was investigated in this work.

EXPERIMENTAL PROCEDURES

Two sets of steel samples with different Si contents were made by vacuum induction melting furnace and cast into ingots which were forged into steel bars, and then hot-rolled into 14 mm thick plates. The chemical compositions of these steels are given in Table 1. The steel plates were normalized at 1000 ºC for 30 min and cooled in furnace, followed by tempering at 650ºC and 700ºC for 180 min and finally quenched in water.

The microstructures of the steels were examined by optical and scanning electron microscopy (SEM). Micrograph analysis was applied to determine the amount of ferrite in the bainite-ferrite microstructure. The composition of alloy carbide was determined using transmission electron microscope (TEM) equipped with energy dispersive spectroscopy (EDS). Thin foils of ~ 300 μm thickness, sliced from bulk specimens using disc cutter, were ground with silicon carbide paper to approximately 50 μm thickness. Electro polishing was conducted using a twin jet electro polisher in a solution containing 10 vol.% perchloric acid and 90 vol% glacial acetic acid. The Vickers hardness tests (0.5kg) were carried out using Buehler Micromet 5101. Each reported hardness value is the average of at least 10 measurements. The transverse V-notch Charpy impact test was carried out at -30 ºC. The reported toughness value is the average of 3 measurements.

RESULTS

Microstructures

Fig. 1 shows the typical microstructure of normalized 0.54 and 1.55 % Si steels after tempering at 650 °C and 700 °C. It is seen that the tempered microstructures consist of bainite (B) and ferrite (F). The ferrite is likely to be formed during cooling from the austenite temperature. Fig. 2 shows SEM micrographs of the same steels tempered at 650 ºC. It can be seen that more and finer carbides are distributed in the matrix of the 0.54 % Si steel compared to those in the 1.55 % Si steel.

Mechanical properties

Table 2 shows the mechanical properties of the tempered Cr-Mo alloyed steels. As the tempering temperature increased from 650 °C to 700 ºC, the average Charpy absorbed energy decreased from 158 to 91 J and 83 to 31 J in the 0.54 and 1.55% Si steels, respectively. Clearly, the 0.54 % Si steel had the higher room and low temperature toughness than the 1.55 % Si steel. The hardness values of both steels were comparable.

Precipitates

Fig. 3 shows the TEM micrographs in which three kinds of alloy carbides, $M_{23}C_6$, M_6C and M_7C_3 (as indicated by the arrows) are identified in the tempered Cr-Mo steels. Spherical particles were identified as M_6C carbides. The M_7C_3 and $M_{23}C_6$ carbides appeared as blocky and elongated plate-like precipitates.

Fig. 4 shows that $M_{23}C_6$ was precipitated in both steels whereas M_6C were found only in 0.54% Si steel and M_7C_3 only in 1.55 % Si steel. Because the precipitates in low-Si and high-Si steel grades have different shape, their size is normalized in area. Their measured equivalent circle areas calculate the radius of particles. 483 particles in the low-Si steel and 396 particles in the high-Si steel were counted, and the size distribution of the particles is shown in Fig. 5. It is seen that as the silicon content increased from 0.54 to 1.55 %, the average size of alloy carbides was increased from 20~30 nm to 40~60 nm.

Fig. 6 shows the effect of silicon content and tempering temperature on the weight percent of alloy carbides as calculated using JMatPro software. It should be noted that the partitioning of carbon among ferrite, austenite and carbide was not considered to simplify the calculation. Clearly $M_{23}C_6$ content is higher in the high-Si steel regardless of the tempering temperature (see Fig. 6). Also, blocky M_7C_3 particles are formed in the high-Si steel whereas equiaxed M_6C precipitates are formed in the low-Si steel.

Fracture surfaces

Fig. 7 shows cleavage-rupture type of failure on all fracture surfaces of the tempered Cr-Mo alloy steels. As the tempering temperature increased from 650 to 700 °C, the cleavage size in both 0.54 and 1.55 % Si steels was sharply increased.

DISCUSSION

The effect of silicon on carbide precipitation and impact toughness

Earliest investigations on the effect of silicon on carbide precipitation were conducted more than 50 years ago [19] and it is a well-proven fact that silicon can inhibit the formation of cementite. In high alloy steels, the precipitation of cementite takes place in the early stage of tempering, affecting the subsequent formation of alloy carbides [20].

Advanced microscopy techniques allow *in-situ* observation of alloy carbides formation. For instance, it is shown that most of alloy carbides nucleate and grow at the cementite/ferrite interface by “extracting” carbon from the adjacent cementite [21]. Consequently, cementite gradually disappears as the alloy carbides continue to grow. In the low Si steel, cementite formation at the early stages was not fully prevented and more stable $M_{23}C_6$ and M_6C carbides formed adjacent to the cementite during long time tempering cycles at 650°C. In contrast, in the 1.55 % Si steel, suppression of cementite formation occurred during tempering, hence, M_7C_3 and $M_{23}C_6$ carbides were nucleated preferentially on the grain boundaries and lattice defects where carbon diffusion rate was higher; resulting in coarser alloy carbides than those in the low Si steel.

Smith model [22] assumes cleavage cracks can initiate when the grain boundary carbide is fractured by the impingement of a dislocation pile-up, and hence the final fracture is controlled by crack propagation into the neighboring ferrite. The size and number of carbide particles are regarded as a major factor controlling cleavage fracture in various steels [23]. It is also shown that an increase in the carbide particle size can lower the fracture toughness over a temperature range from -200 to -50 ºC [24]. In the present work, it is proposed that the numerous coarse carbides in the higher Si steel provided preferential sites for the nucleation of cleavage facets, in the tempered microstructures, which attributed to the formation of micro-voids and cleavage type fracture. However, the dispersion of alloy carbide particles in the lower Si resulted in a higher toughness at low temperatures. Similar phenomena were reported when tempering Nb-Ti micro-alloyed cryogenic pressure vessel steels [18]. It was demonstrated that silicon content had remarkable influence on the precipitated alloy carbide size. Consistently, the low temperature impact absorbed energy of the low Si steel was higher than that of the high Si steel [18].

The effect of silicon on microstructure and impact toughness

In bainite-ferrite dual phase steels, ductile ferrite (~ 4 vol.%) can retard propagation of micro-cracks and consequently increases resistance to the brittle fracture. It is argued that the presence of a ductile phase in the vicinity of bainite has stress-relief effect ahead of propagating cracks [25]. In contrast, it has been reported that the fractured toughness was decreased when the ferrite volume fraction exceeded 20% [26]. The outcome of this work supported the former, since as the tempering temperature increased from 650 to 700 ºC, the ferrite volume fraction in the 0.54 and 1.55 % Si steels increased up to 24.1 and 39.3 vol.% (see Table 3), respectively; resulting in reduction in the low temperature toughness of both steels.

CONCLUSIONS

(1) The mixed microstructures of bainite and ferrite were obtained in the normalised then tempered Cr-Mo alloyed steels with different Si contents.

(2) The low temperature toughness can be enhanced by reduction of the silicon content in the Cr-Mo alloyed steels.

(3) It was shown that silicon can change the nature and distribution of subsequent alloy carbides by affecting the precipitation of cementite in the earlier stages of tempering.

ACKNOWLEDGEMENTS

The authors gratefully acknowledge the financial support from Wuhan International Science and Technology Corporation Program (No. 2014030709020307).

REFERENCES

[1] C. J. Moss, P. M. Kelly, Fatigue Fract. Eng. Mater. Struct., **17**, 369 (1994).

[2] J. H. Bulloch, Int. J Pres. Ves. Pip., **58**, 231(1994).

[3] S. M. Bruemmer, Corros Sci., **44**, 364(1988).

[4] T. Iwadate, Y. Tanaka, H. Takemata, J Press Vess. T, **116**, 353 (1994).

[5] C. A. Hippsley, Mater. Sci. Technol., **1**, 475 (1985).

[6] N. S. Cheruvu, Metall. Mater. Trans. A, **20**, 87 (1989).

[7] Z. Qu, C. J. McMahon, Metall. Mater. Trans. A, **14**, 1101 (1983).

[8] R. Pilkington, R. Dicken, P. Peura, G. W. Lorimer, et al., Mater. Sci. Eng. A, **212**, 191 (1996).

[9] R. L. Bodnar, T. Ohhashi, R. I. Jaffee, Metall. Mater. Trans. A, **20**, 1445 (1989).

[10] Y. Nishizaka, Y. Hara, A. Hori, H. Tsukahara, et al., J Press Vess. Tech., **107**, 285 (1985).

[11] J. Yu and C. J. McMahon, Metall. Mater. Trans. A, **11**, 291 (1980).

[12] A. Gustafson and A. John, ISIJ Int., **41**, 356 (2001).

[13] H. K. D. H. Bhadeshia and R. W. K. Honeycombe, *Steels microstructure and properties, Third edition*, Elsevier Ltd., Oxford (2006), pp. 183-197.

[14] W. S. Owen, Trans. ASM, **46**, 812 (1954).

[15] K. Maruyama, K. Sawada, J. Koike, ISIJ Int., **41**, 641 (2001), No. 6, p. 641.

[16] D. Delagnes, P. Lamesle, M. H. Mathon, et al., Mater. Sci. Eng. A, **394**, 435 (2005).

[17] R. A. Mesquita, H. J. Kestenbach, Mater. Sci. Eng. A, **528**, 4856 (2011).

[18] J. A. Qiu, K. M. Wu, J. H. Li, et al., Mater. Char., **83**, 123 (2013).

[19] J-MatPro 4.0, http://www.cntech.com.cn/product/JMatPro.html.

[20] W. S. Owen, Trans. ASM, **46,** 812 (1954).

[21] W. M. Garrison, Mater. Sci. Technol., **3**, 256 (1987).

[22] J. V. Bee, P. R. Howell, R. W. K. Honeycombe, Metall. Mater. Trans. A, 10, 1207

(1979).

[23] E. Smith, “Physical basis of yield and fracture”, in: *Proc. Institute of Physics and Physical Society*, Oxford, United Kingdom, 1966, pp. 26-57.

[24] P. Bowen, S. G. Druce, J. F. Knott, Acta Metall., **34**, 1121 (1986).

[25] S. Ortner, Int. J Pres. Ves. Pip., **79**, 693 (2002).

[26] M. Khakian, *MSc thesis*, Sharif University of technology, (2006).

[27] M. E. Hanno, *MSc thesis*, Royal Institute of Technology (KTH), (2012).

TABLE 1. Chemical composition (wt.%) of the Cr-Mo alloyed steels used in this work.

Steels	C	Si	Mn	Cr	Mo	Ni	P	S	Fe
0.54 % Si	0.12	0.54	0.49	1.20	0.49	0.14	0.007	0.004	Bal.
1.55 % Si	0.13	1.55	0.50	1.14	0.45	0.13	0.005	0.003	Bal.

TABLE 2. Mechanical properties of the normalized-tempered Cr-Mo alloyed steels used in this work.

Steels	Charpy absorbed energy, J (-30 ºC)		HV0.5
	650 ºC	700 ºC	
0.54 % Si	100, 160, 213, <u>158</u>	122, 74, 76, <u>91</u>	232.9 ± 7.5
1.55 % Si	77, 78, 94, <u>83</u>	12, 54, 28, <u>31</u>	239.1 ± 10.2

TABLE 3. Measured volume fraction of ferrite in low and high Si steels *vs.* the tempering temperature.

Steels	Ferrite volume fraction, %	
	650 ºC	700 ºC
0.54 % Si	15.5	24.1
1.55 % Si	16.9	39.3

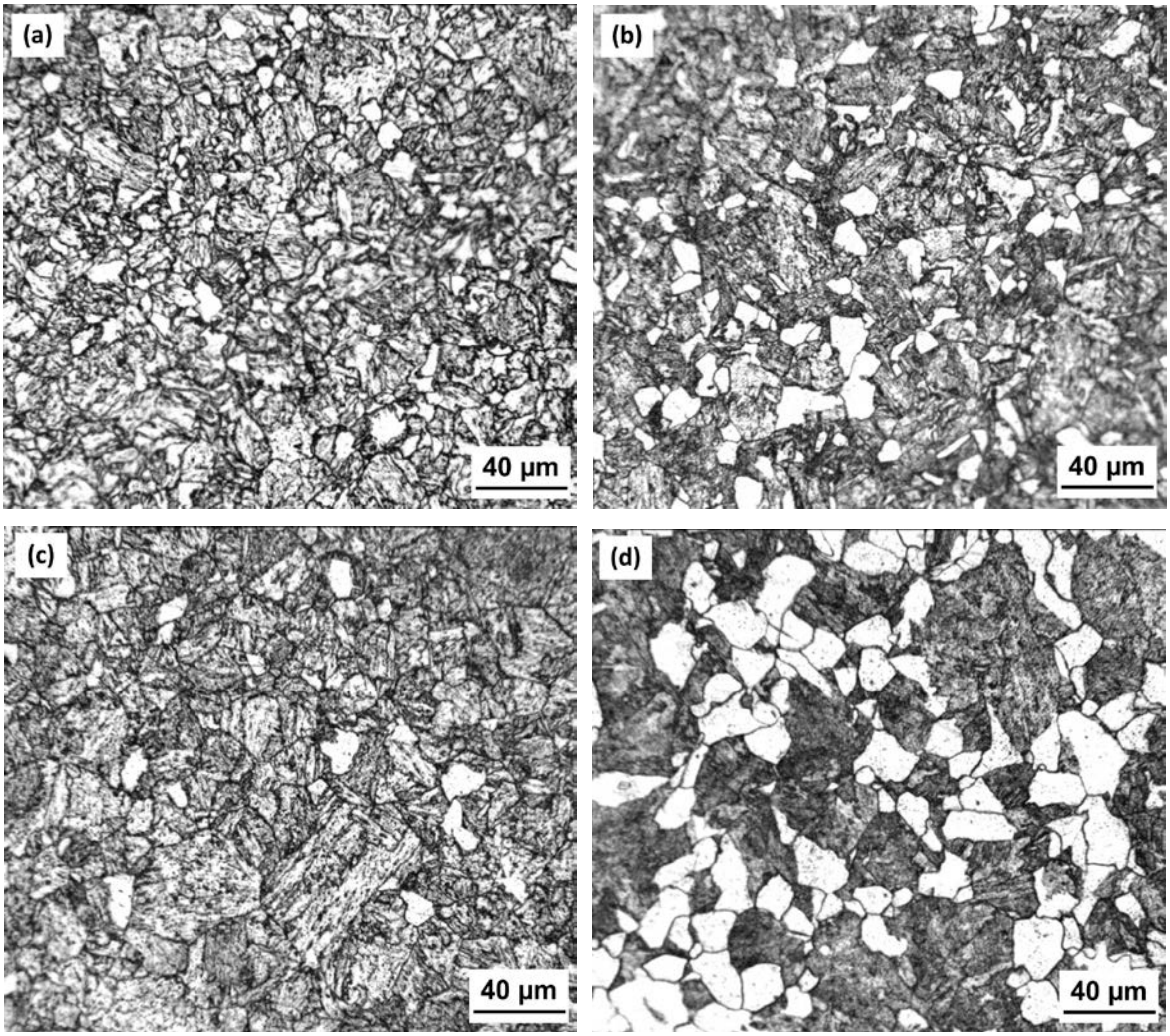

Fig. 1. Optical micrographs of tempered Cr-Mo alloyed steels (a) 0.54 % Si, 650 ^{o}C, (b) 1.55 % Si, 650 ^{o}C, (c) 0.54 % Si, 700 ^{o}C, (d) 1.55% Si, 700 ^{o}C.

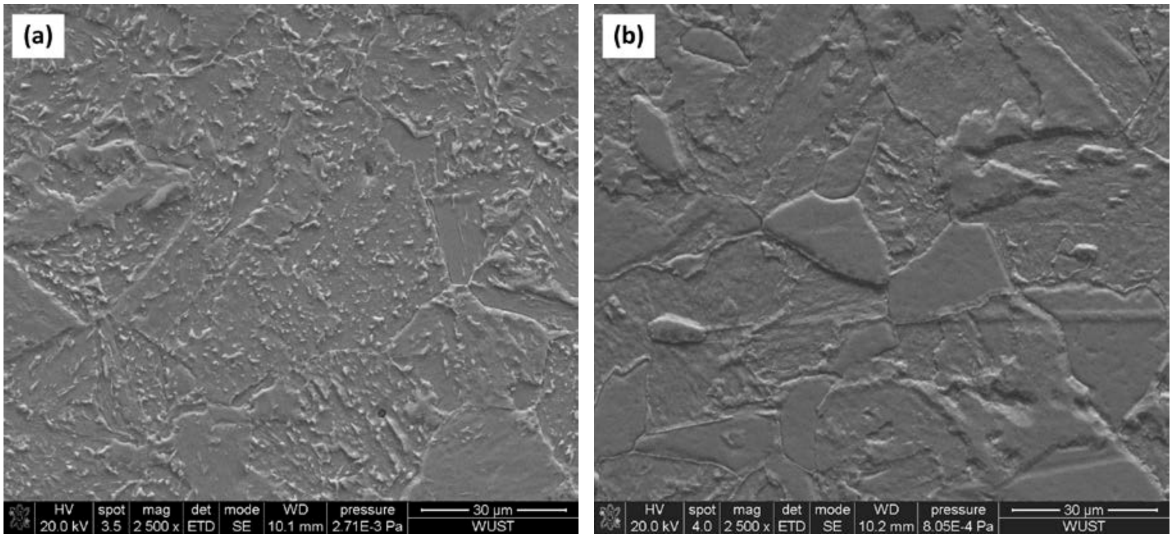

Fig. 2. SEM micrographs of steel samples tempered at 650 ℃ (a) 0.54 % Si, (b) 1.55 % Si.

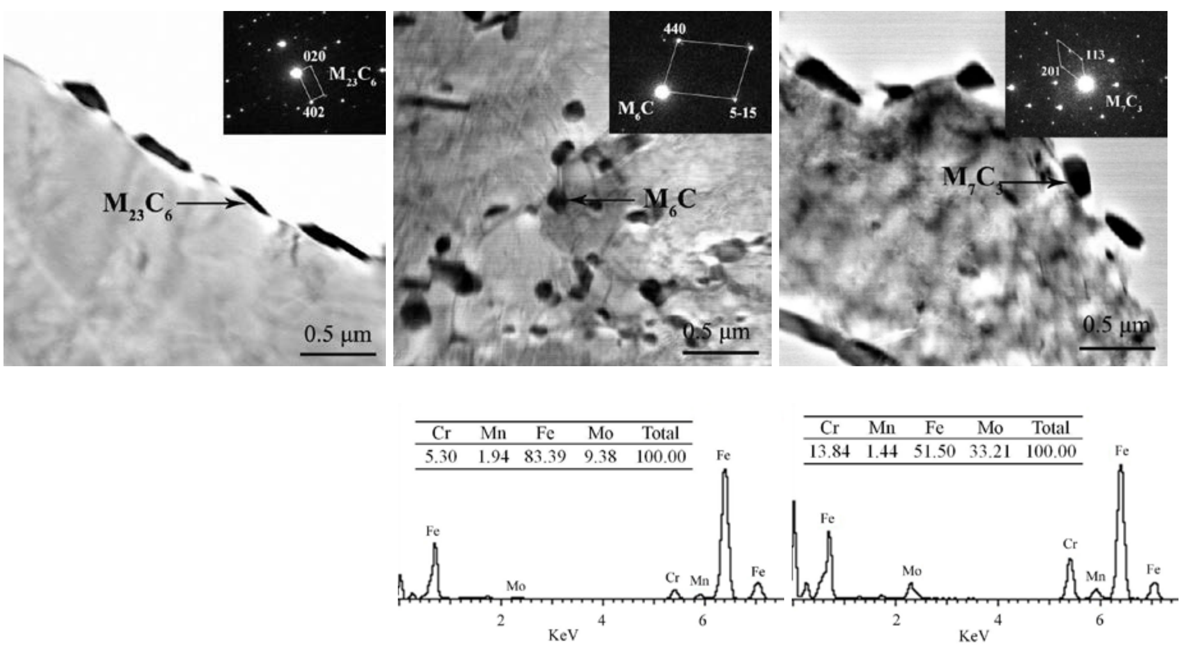

Fig. 3. TEM micrographs of various carbides and corresponding EDS results

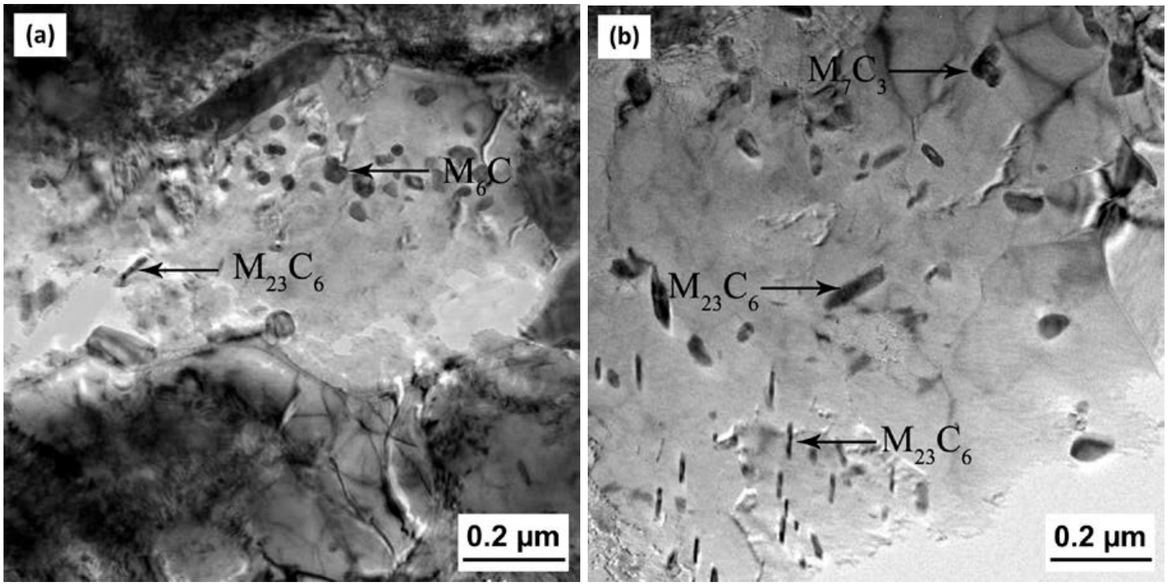

Fig. 4. TEM micrographs of precipitates in (a) 0.54 % Si and (b) 1.55 % Si steels

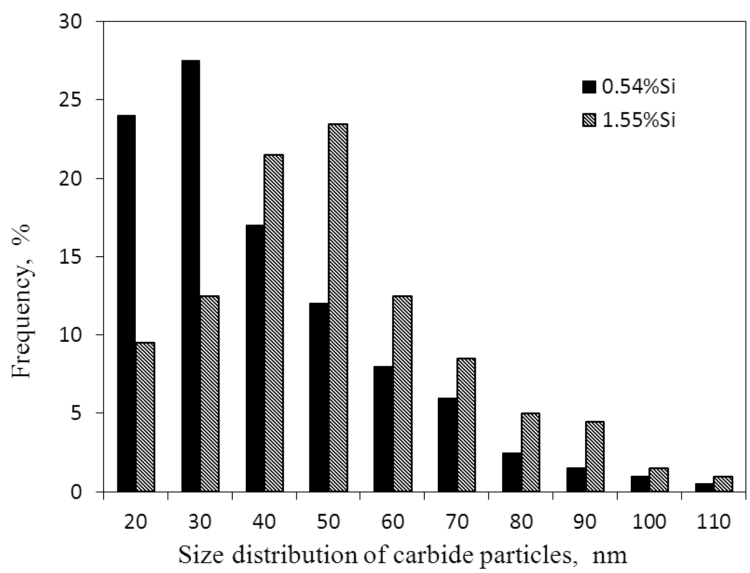

Fig. 5. Size distribution of alloy carbide particles: comparison between the high silicon and low silicon steels grades.

Fig. 6. Carbide contents *vs.* tempering temperature calculated using JMatPro software.

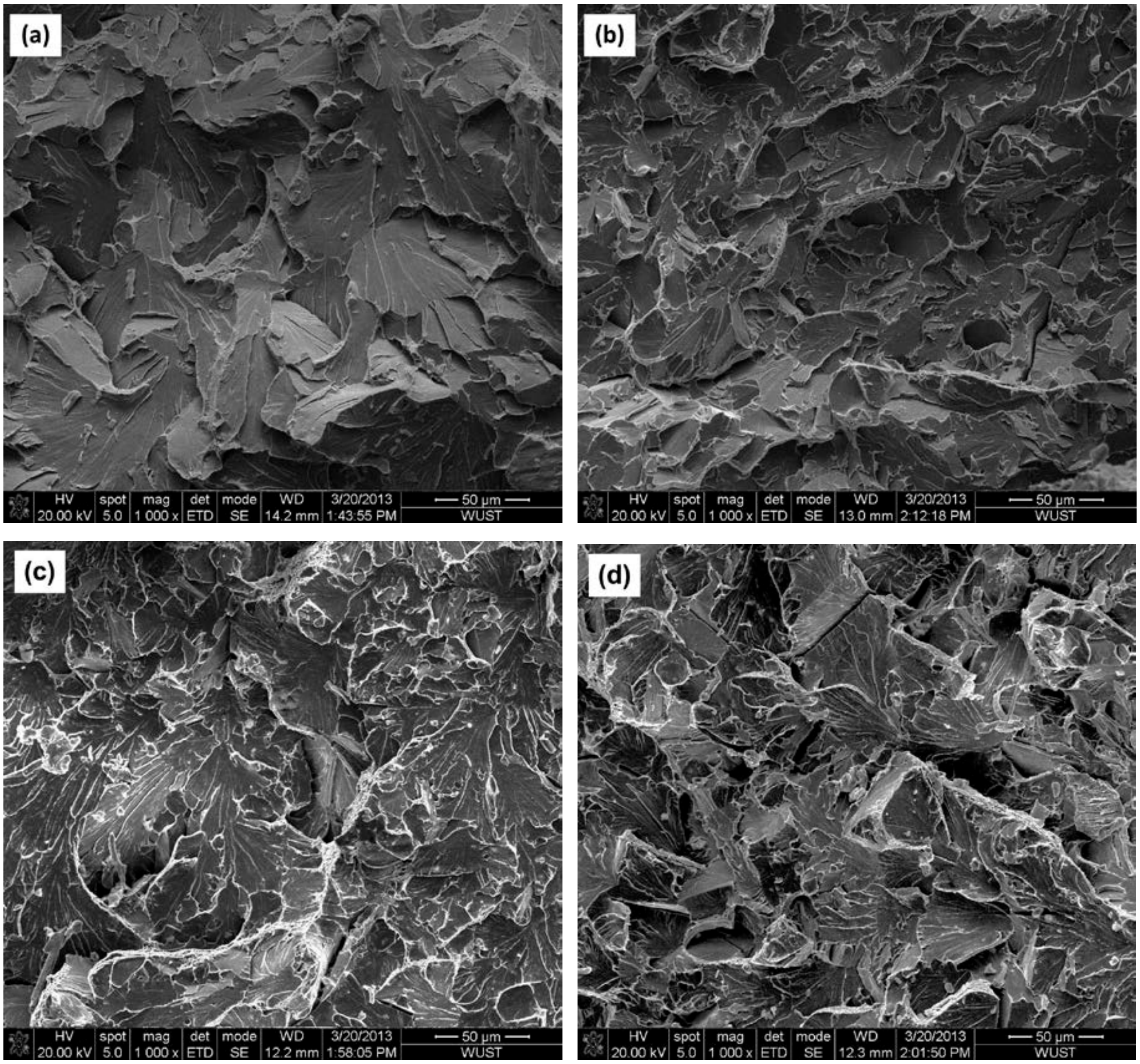

Fig. 7. Fracture surfaces (-30 ℃) of normalized-tempered Cr-Mo alloyed steels (a) 0.54 % Si, 650 ℃, (b) 1.55 % Si, 650 ℃, (c) 0.54 % Si, 700 ℃, (d) 1.55% Si, 700 ℃